Convective condensation of R134a and R1234ze(E) inside microfin tube

Convective condensation of R134a and R1234ze(E) inside microfin tube

A Lucchini[1], I M Carraretto[1], T N Phan[2,3], P G Pittoni[4], L Molinaroli[1] and L P M Colombo[1]

[1] Politecnico di Milano, Department of Energy, via Lambruschini 4, 20156 Milano, Italy
[2] Ho Chi Minh City University of Technology (HCMUT), 268 Ly Thuong Kiet Street, District 10, Ho Chi Minh City, Vietnam
[3] Vietnam National University Ho Chi Minh City, Linh Trung Ward, Thu Duc District, Ho Chi Minh City, Vietnam
[4] Iowa State University, 2529 Union Drive, Ames, IA 50011, United States

andrea.lucchini@polimi.it

Abstract. Environmental concerns are forcing the replacement of the commonly used refrigerants and finding new fluids is a top priority. The hydro-fluoro-olefin (HFO) R1234ze(E), because of its smaller global warming potential (GWP) and shorter atmospheric lifetime, replaced R134a. Accordingly, for HVAC systems design, a detailed knowledge of the thermo-fluid-dynamic characteristics of the fluids and reliable predictive models are required. To improve the understanding, R134a and R1234ze(E) were employed in convective condensation experiments (saturation temperature T_{sat} = 35°C, mean quality x_m = 0.1~0.9, quality changes Δx = 0.05~0.6, mass flux G = 43~444 kg·m^{-2}s^{-1}) inside a microfin tube (outer diameter D = 9.52 mm, fin number n = 60, fin height H = 0.2 mm). The results were used for two goals: the former is the comparison of the heat transfer features of the two fluids, while the latter aims at testing the performance of prediction models available in the open literature. At the saturation temperature T = 35°C, the two fluids show small differences in the thermal properties so that, as expected, the experiments highlighted a very similar behavior in the typical operating conditions of HVAC systems. In fact, for all the operating conditions marginal differences were observed in the pressure drop, the heat transfer coefficient and the flow pattern maps. The issue of prediction reliability, however, is still open. Actually, not all the models achieving good results for R134a show the same performance for R1234ze(E), especially for the pressure drop.

1. Introduction

The European Parliament developed a strategy to shift to a competitive low carbon economy. Accordingly, the European Regulation (EU) No. 29 517/2014 [1] prescribes the phase-out steps for the HFC. To properly design the next generation HVAC devices the search for new refrigerants is a top priority. The hydro-fluoro-olefin (HFO) R1234ze(E) seems a good replacement for R134a because of its environmental features: short atmospheric lifetime (17 days for R1234ze(E), 13.8 years for R134a [2]) and small global warming potential (less than 1 for R1234ze(E), 1430 for R134a [2]). Nevertheless, a negative impact on the overall performance, mostly due to vapor compression efficiency is reported as drawbacks [3]. The performance variation and its assessment were the main

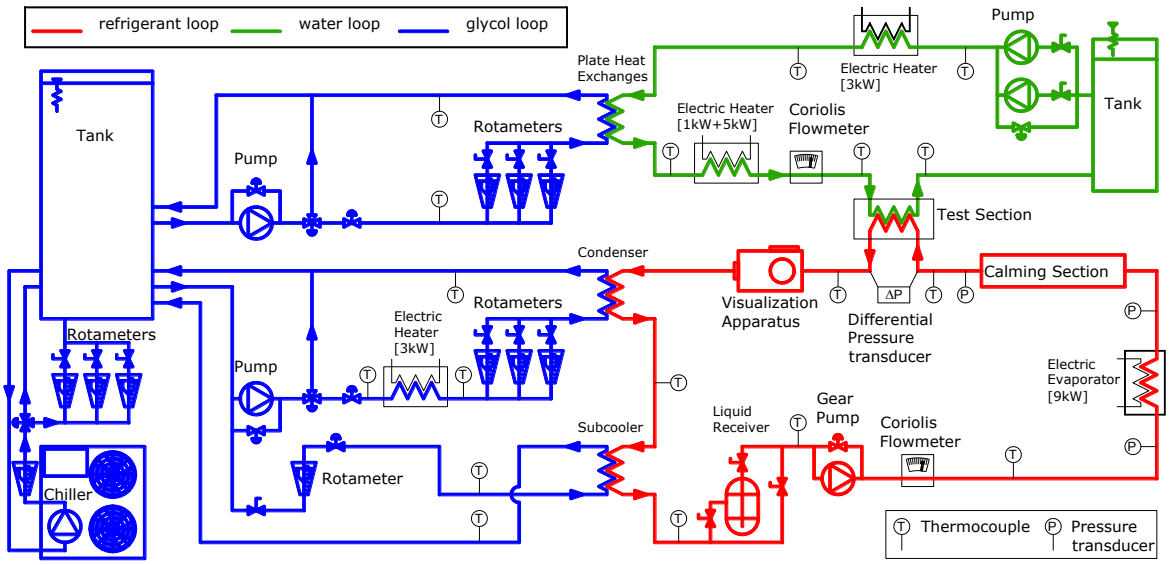

Figure 1. Experimental apparatus

concerns of the researcher in the last few years. The topics were approached at two different levels: the process (thermodynamics, transport phenomena), and the energy system. An example about the latter topics is provided by Censi and Padovan [3]: they examined a Microfin Shell-and Tube Evaporator, even though the overall heat transfer coefficient was almost unchanged, it was reported a 25% lower heat transfer rate for R1234ze(E) due to the same reduction in the volume flow rate. Colombo et al. [4] provided a further case, reporting a reduction up to 12.3% in the COP of a water-to-water heat pump compared to R134a. Zhang [5] highlighted, for a plate heat exchanger, that the HFOs refrigerants, compared to their HFC counterparts, show higher heat transfer coefficients and pressure drops when operating under the same conditions.

To correctly design HVAC components and systems, it is of paramount importance the availability of both experimental data, reporting the heat transfer characteristics of the new fluids, and reliable correlations capable for their predictions. This work compares the heat transfer performance, namely the pressure drop per unit length and the heat transfer coefficient, of R134a (reference fluid) and R1234ze(E) (drop-in replacement) during convective condensation in horizontal microfin tubes. Experimental data were compared with the prediction provided by well-known correlations developed to estimate the pressure drop per unit length [6 – 13] and the heat transfer coefficient [14 – 16].

2. Experimental apparatus

The experimental apparatus (Figure 1) is made of three main circuits (their detailed description is reported in [17]) named: the refrigerant loop (filled initially with R134a and then with R1234ze(e)), the water loop (filled with demineralized water) and glycol loop (filled with a mixture of water and ethylene glycol, 30% volume concentration).

2.1. The glycol loop

The glycol loop (blue line in Figure 1) has two main tasks: to set the operating temperature in the test section (fixing the pressure in the condenser) and to chill both refrigerant and water. A commercial chiller cools the mixture to -10°C and then it is stored in a 0.75 m^3 tank. Two independent loops, one for the water and the other for the refrigerant, are connected to the tank.

The former loop cools the water entering in the test section, which heats up because of the viscous dissipation. The other loop is in charge to set the temperature in the test section and to prevent cavitation in the refrigerant pump. The former operation is accomplished setting the mass flow rate and the temperature at the condenser inlet, using a P.I.D. driven electric heater, such that the

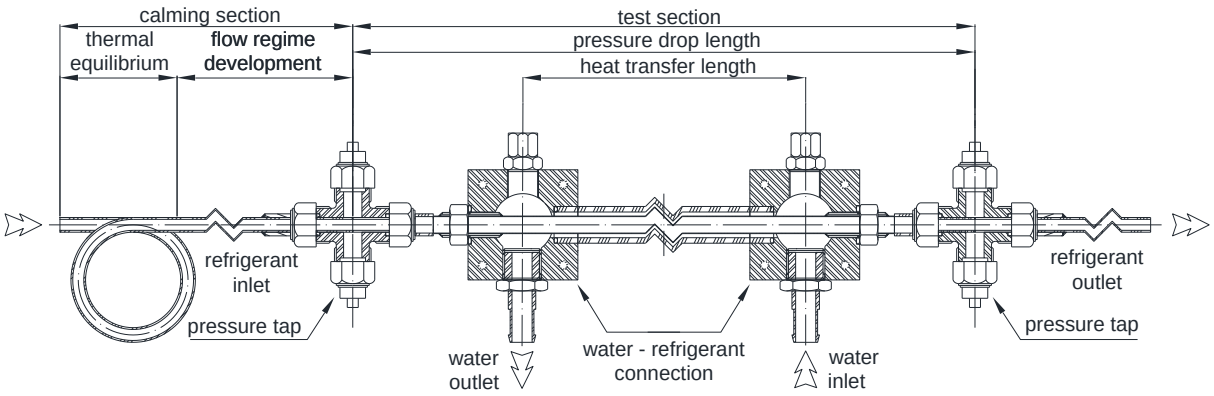

Figure 2. Test section

refrigerant pressure at the test section inlet be the saturation pressure corresponding to the test temperature. For the latter operation a bypass drains part of the mixture headed to the condenser to subcool the refrigerant entering the pump.

2.2. The water loop

The water loop (green line in Figure 1) is designed to exchange the thermal power required for the refrigerant phase change. The heat transfer takes place in a tube in tube heat exchanger (water in the annulus, refrigerant in the inner duct), named test section (Figure 2), thermally insulated from the surroundings. A pump drains the water from the tank, the mass is measured by a Coriolis flowmeter (range [0;400] kg/h, uncertainty 0.15% of the reading). Afterwards the flow enters in a plate heat exchanger, then a P.I.D. driven electric heater sets the inlet temperature in the test section such that the power transfer causes a -2°C temperature reduction of the water flow, two groups of 3 K-type thermocouples connected in series (uncertainty 0.1K) measure the inlet and outlet temperature.

2.3. The refrigerant loop

The main goal of the refrigerant loop (red line in Figure 1) is to provide, at the inlet of the test section (where the measures take place), a two-phase flow of refrigerant at specified operating conditions, they are defined by: mass flow rate, inlet quality and the inlet temperature.

A saturated liquid flow of refrigerant leaves the condenser and enters in a plate heat exchanger (subcooler) to prevent cavitation in the pump (gear type with inverter driven engine for the mass flow rate tuning). A Coriolis flowmeter (range [0;400]kg/h, uncertainty 0.15% of the reading) records the mass flow rate while a pressure transducer (relative, range [-1;30] bar, uncertainty ±1% of full scale) and a thermocouple (K-type, uncertainty 0.1K) check the thermodynamic state of the refrigerant as it enters in the evaporator, which provides the power to vaporize the amount of refrigerant specified by the test section inlet quality. A calming section (Figure 2) follows, it is made of two parts: a wrapped tube (to get the thermal equilibrium between liquid and vapor) and a straight duct (to get fully developed flow regime). Then the refrigerant enters in the test section and returns to the condenser.

The test section (Figure 2) has a heat transfer length L=1.11 m and is thermally insulated with 10 cm thick rubber foam shell. The geometrical features of the cross-section are listed in Table 1.

A differential pressure transducer (range [-103.4;103.4] kPa, uncertainty ±0.1% of the full scale), connected to two pressure taps separated by the distance l=1.3 m, records the pressure drop. While a relative pressure transducer (range [-100;1600] kPa, uncertainty ±0.25% of the full scale), connected to the tap at the inlet of the test section, reads the refrigerant pressure. The refrigerant inlet and outlet temperatures are the saturation temperatures given by the pressure readings. Two groups (one at the entrance and one at the exit) of three thermocouples are glued inside grooves (length 50 mm, depth 0.15 mm, width 0.4 mm) on the outside of the tube (top, side and bottom position), to measure the wall temperatures. The reference junction of each thermocouple (K-type, uncertainty 0.1K) is inserted in a Dewar flask filled with melting ice.

Table 1. Microfin tube J60 geometrical features

tube				cross-section			
Outer diameter		[mm]	9.52	Wet perimeter		[mm]	44.9
Fin-root diameter	D_R	[mm]	8.96	Cross section area	A	[mm^2]	62.2
Fin number	n	[-]	60	Hydraulic diameter		[mm]	5.28
Height	H	[mm]	0.2	Exchanging area ratio		[-]	1.68
Apex angle	α	[°]	40				
Helix angle	β	[°]	18				

3. Data reduction

Data processing aims at computing the quantities that identify the experimental operating conditions (saturation temperature at the test section inlet T_{ri}, mass flux G, quality change in the test section Δx, average quality in the test section x_m), the pressure drop per unit length Z and the heat transfer coefficient h. A datapoint is picked for each experimental condition, it is the average of 12 acquisitions and each of them is the mean value of 181 samples (1 Hz sampling for 3 minutes).

Preliminary checks on the thermal insulation, performed using single phase vapor flow, showed that the power transferred, computed for both refrigerant side and water side, matched within 5%.

The inlet and outlet refrigerant temperatures are the saturation temperatures corresponding to the inlet and the outlet pressure, the former is measured by a relative pressure transducer while the latter is computed subtracting to the inlet pressure the pressure drop on the test section provided by a differential pressure transducer.

$$T_{\mathrm{ri}} = T_{\mathrm{sat}}(p_{\mathrm{ri}}) \tag{1}$$

$$T_{\mathrm{ro}} = T_{\mathrm{sat}}(p_{\mathrm{ri}} - \Delta p) \tag{2}$$

Referring to the nominal geometrical features of the microfin tube, the net cross section area is:

$$A_{\mathrm{c}} = \frac{\pi D_{\mathrm{r}}^2}{4} - \frac{nH^2}{\cos\beta}\tan\left(\frac{\alpha}{2}\right) \tag{3}$$

From the Coriolis flowmeter reading, the refrigerant mass flux is computed as follows:

$$G = \frac{\dot{m}_{\mathrm{r}}}{A_{\mathrm{c}}} \tag{4}$$

Assuming steady state and negligible thermal dispersion in the test section, the power transfer takes place only between water and refrigerant:

$$\dot{Q} = \dot{m}_{\mathrm{a}} c_{\mathrm{pa}} (T_{\mathrm{ai}} - T_{\mathrm{ao}}) \tag{5}$$

The quality change can be computed as:

$$\Delta x = (x_{\mathrm{o}} - x_{\mathrm{i}}) = \frac{\dot{Q}}{\dot{m}_{\mathrm{r}} h_{\mathrm{lv}}(p_{\mathrm{ri}})} \tag{6}$$

The inlet quality can be determined performing an energy balance on the evaporator, assuming steady state and negligible thermal dispersion:

$$x_{\mathrm{i}} = \frac{\dot{Q}_{\mathrm{e}} - \dot{m}_{\mathrm{r}} c_{\mathrm{pr}} [T_{\mathrm{sat}}(p_{\mathrm{rei}}) - T_{\mathrm{rei}}]}{\dot{m}_{\mathrm{r}} h_{\mathrm{lv}}(p_{\mathrm{ri}})} \tag{7}$$

In the end the mean quality in the test section is:

$$x_{\mathrm{m}} = x_{\mathrm{i}} + \frac{\Delta x}{2} \tag{8}$$

The total pressure drop per unit length is computed as the ratio of the total pressure drop Δp to the distance l between the pressure taps (measured at the end of the building process).

$$Z = \frac{\Delta p}{l} = \frac{p_{ri} - p_{ro}}{l} \tag{9}$$

The average heat transfer coefficient h is based on the logarithmic mean temperature between wall and refrigerant temperatures. The former is the mean of the readings provided by the three thermocouples on the outside of the tube, such that logarithmic mean temperature difference is

Table 2. Experimental operating conditions

quantity	T_{ri} [°C]	G [kg·m^{-2}·s^{-1}]	x_m [-]	Δx [-]	q [kW·m^{-2}]
range	35±0.1	[43;442]	[0.10;0.91]	[-0.63;-0.05]	[-45.7;-3.5]

$$T_{\mathrm{w}} = \frac{T_{\mathrm{t}} + T_{\mathrm{s}} + T_{\mathrm{b}}}{3} \tag{10}$$

$$\Delta T_{\mathrm{ml}} = \frac{(T_{\mathrm{wo}} - T_{\mathrm{ro}}) - (T_{\mathrm{wi}} - T_{\mathrm{ri}})}{\ln \frac{T_{\mathrm{wo}} - T_{\mathrm{ro}}}{T_{\mathrm{wi}} - T_{\mathrm{ri}}}} \tag{11}$$

The heat transfer area of the refrigerant duct refers to the fin root diameter, hence the heat flux is:

$$q = \frac{Q}{\pi D_{\mathrm{i}} L} \tag{12}$$

Finally, the average heat transfer coefficient in the test section is given by the following equation:

$$h = \frac{q}{\Delta T_{\mathrm{ml}}} \tag{13}$$

The propagation uncertainty analysis (further details can be found in [17]) showed that, for each datapoint, the uncertainty related to the parameters identifying the operating conditions, the pressure drop per unit length and the heat transfer coefficient is lower than 5%.

4. Experimental results

The experiments aimed to compare the heat transfer features, during convective condensation (operating condition in Table 2), of R134a, the reference fluid, and its drop-in replacement R1234ze(E). Some preliminary remarks concerning the main differences in the thermal properties of the fluids, at the saturation temperature, are useful to understand the results (Table 3 and Table 4).

A. R1234ze(E) has 5.4% smaller phase change enthalpy than R134a, it means that, for the same quality change, the R1234ze(E) flow requires a smaller thermal power. As the experiments were performed in the same test section, the same statement holds for the heat flux too. Conversely, for a fixed heat flux, the quality change for the R1234ze(E) flow is larger.
B. R1234ze(E) has 19% smaller vapor density than R134a, it follows that, at the same mass flux, the R1234ze(E) flow has a higher mean velocity than the R134a flow.
C. R1234ze(E) shows a liquid thermal conductivity about 8% smaller than R134a. Accordingly, for the same heat flux in shear dominated flows, the logarithmic mean temperature difference for R1234ze(E) is larger than the one for R134a because, the difference between the bulk temperature and the wall temperature is larger for the R1234ze(E) flow.
D. Comparable frictional pressure drop could be expected, between R134a and R1234ze(E), because the differences in the liquid and vapor dynamic viscosities are smaller than 6%.

4.1. Complete condensation

During convective condensation the total pressure drop is the algebraic sum of a positive term related to viscous dissipation, the frictional pressure drop, and a negative term connected to the bulk velocity reduction, the accelerative pressure drop. According to Figure 3, R1234ze(E) and R134a have

Table 3. Liquid and vapor thermal properties of R134a (reference fluid) and R1234ze(E) at saturation temperature T_{ri}=35°C (source: RefProp 10)

		R134a		**R1234ze(E)**	
$p_{sat}(T_{ri})$	[MPa]	0.887		0.667	
h_{lv}	[kJ·kg^{-1}]	1.682·10^{2}		1.590·10^{2}	
		Liquid	**Vapor**	**Liquid**	**Vapor**
ρ	[kg·m^{-3}]	1.168·10^{3}	4.342·10^{1}	1.129·10^{3}	3.527·10^{1}
c_p	[kJ·kg^{-1}K^{-1}]	1.471	1.103	1.422	1.023
k	[W·m^{-1}·K^{-1}]	7.685·10^{-2}	1.490·10^{-2}	7.085·10^{-2}	1.450·10^{-2}
M	[Pa·s]	1.720·10^{-4}	1.210·10^{-5}	1.680·10^{-4}	1.280·10^{-5}

Table 4. Variation of the thermal properties.

	$\Delta_{\%}=g/g_{ref}-1$	
$\Delta p_{sat\%}$	-24.8%	
$\Delta h_{lv\%}$	-5.4%	
	Liquid	**Vapor**
$\Delta\rho_{\%}$	-3.3%	-18.8%
$\Delta c_{p\%}$	3.3%	-7.2%
$\Delta k_{\%}$	-7.8%	-2.7%
$\Delta\mu_{\%}$	2.3%	5.9%

comparable frictional pressure drop per unit length, as suggested by remark D. The ratio of the accelerative term (void fraction computed using Zivi's correlation) to the frictional one is, for R1234ze(E), between 30% and 40% and between 25% and 30% for R134a because of the explanation given in remark B. The heat transfer coefficients (Figure 4) are similar too. The larger values recorded for R134a could be related to its larger enthalpy of phase change and liquid thermal conductivity, as indicated in remarks A and C.

4.2. Partial condensation

To remove the effect on the heat transfer coefficient of the difference in the phase change enthalpy, partial condensation tests were performed fixing the heat flux instead of the quality change. For the mass fluxes taken into account, according to [18], shear dominated flow regimes onsets for both the fluids. As highlighted by remark D, R134a and R1234ze(E) share similar frictional pressured drop (Figure 5) for a wide range of mass fluxes, the differences are smaller than 10%. In these operating conditions, the accelerative pressure drop provides a small contribution to the total pressure drop: in absolute terms, its ratio to the frictional pressure drop is less than 15% for both the fluids.

The experiments performed fixing the heat flux (q=15.3kW·m^{-2}) displayed that the two fluid have

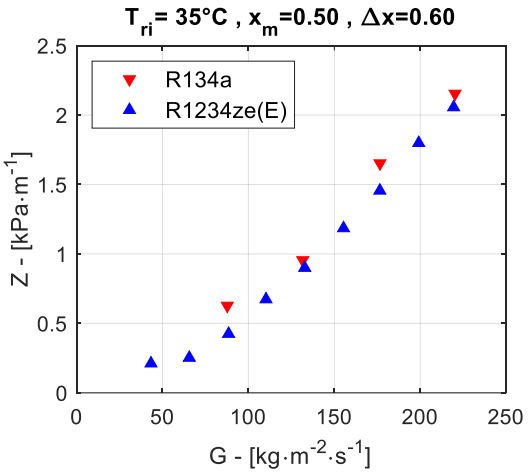

Figure 3. Frictional pressure drop per unit length as a function of mass flux.

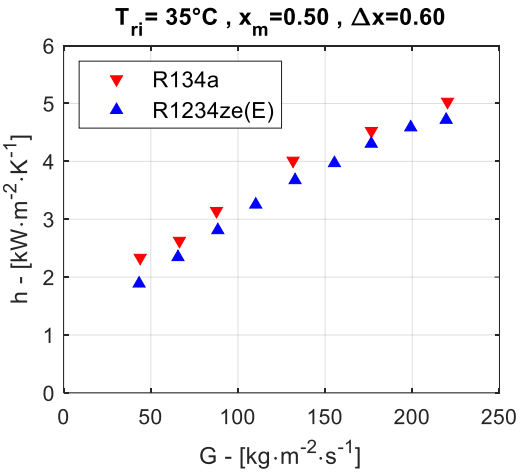

Figure 4. heat transfer coefficient as a function of mass flux.

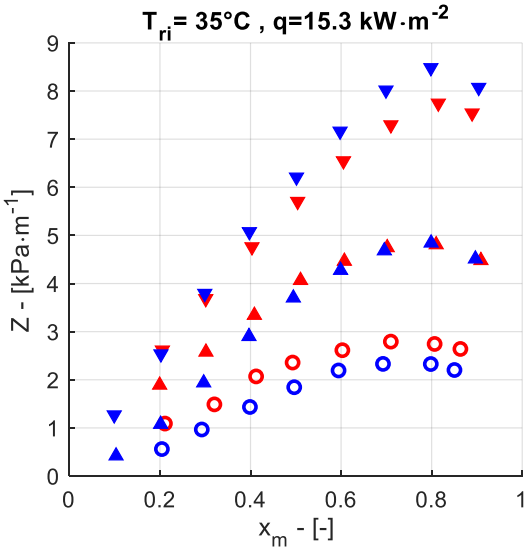

Figure 5. Frictional pressure drop per unit length as a function of mean quality (G_1=220 kg·m^{-2}·s^{-1}, G_2=330 kg·m^{-2}·s^{-1}, G_3=440 kg·m^{-2}·s^{-1}).

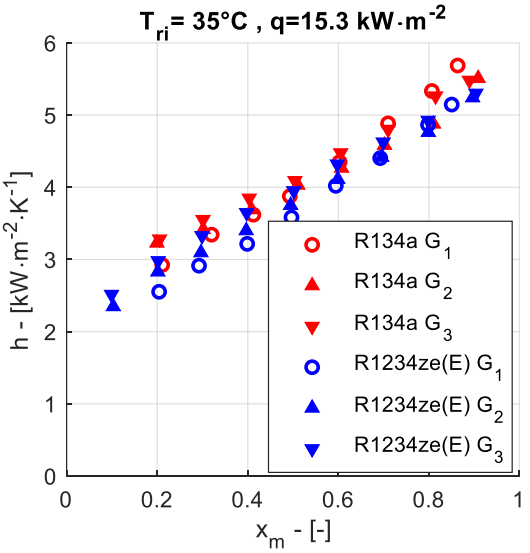

Figure 6. Heat transfer coefficient as a function of mean quality (G_1=220 kg·m^{-2}·s^{-1}, G_2=330 kg·m^{-2}·s^{-1}, G_3=440 kg·m^{-2}·s^{-1}).

Table 5. Comparison between data and the best performing correlations ($E_{\%} \leq 30\%$).

	R1234ze(E)			R134a		
Pressure drop	**$E_{\%}$**	**$E_{A\%}$**	**s**	**$E_{\%}$**	**$E_{A\%}$**	**s**
Domanski [6]	10.5%	30.9%	42.9%	-23.2%	30.9%	33.2%
Kedzierski&Goncalves [13]	-0.4%	27.0%	39.1%	-30.0%	33.9%	30.5%
Shannak [9]	16.2%	36.1%	50.9%	-20.6%	32.6%	36.8%
Muller [19]	10.7%	31.1%	45.9%	-25.1%	32.4%	32.9%
Heat transfer coefficient	**$E_{\%}$**	**$E_{A\%}$**	**s**	**$E_{\%}$**	**$E_{A\%}$**	**s**
Koyama [15]	22.3%	37.3%	49.2%	18.6%	35.1%	46.9%
Kumar&Mohseni [14]	-25.5%	26.1%	13.4%	-24.4%	25.2%	13.6%
Kedzierski&Goncalves [13]	16.8%	27.3%	33.3%	18.5%	26.6%	31.6%

similar heat transfer coefficient (Figure 6), nevertheless R134a shows higher heat transfer coefficients than R1234ze(E) because of its larger liquid thermal conductivity (remark C).

4.3. Comparison between experimental data and correlation

Many different operating conditions were tested, namely 102 for R134a and 122 for R1234ze(E), to properly benchmark the correlations available in the open literature. The pressure drop data were compared with the predictions of 8 correlations [6 – 13]. Only the four in Table 5 provide predictions with a percentage error lower than 30% for both the fluids, nevertheless the performances change a lot for the two fluids. It seems that the available correlations need further tuning to properly account for the effect of the thermal properties and the flow regimes. On the contrary, the predictive models for the heat transfer coefficient seem to work properly. Four correlations [14 – 16] were analyzed and three (Table 5) of them show both a mean percentage error smaller than 30% and similar performances for both the fluids.

5. Conclusions

The experiments point out that the two fluids have similar frictional pressure drop and heat transfer coefficient, the slightly higher values of the latter quantity for R134a are related to its larger thermal properties: phase change enthalpy, liquid and vapor thermal conductivity.

Correlations for the heat transfer coefficient seems to be reliable for both the fluids while the same does not hold for pressure drop. Even though there are models providing, for both the fluids, mean errors smaller than 30% are available their performances are quite different for the two fluids. The issue of prediction reliability, however, is still open, not all the models achieving good results for R134a show the same performance for R1234ze(E), especially for the pressure drop.

Acknowledgments: The authors with gratitude thank Professor Adriano Muzzio for the precious support he gave in developing the experimental apparatus and performing the experiments.

Funding: Research funded by MIUR through the program PRIN 2015, grant number 2015M8S2PA.

Nomenclautre

Latin symbols

A	cross sectional area [m^2]	l	distance between the pressure taps [m]
c_p	specific heat capacity [$J \cdot kg^{-1} \cdot K^{-1}$]	L	heat transfer length [m]
D	diameter [m]	m	mass flow rate [$kg \cdot s^{-1}$]
$E_{\%}$	mean percentage error [-]	n	fin number [-]
$E_{A\%}$	mean absolute percentage error [-]	p	refrigerant pressure [Pa]
G	refrigerant mass flux [$kg \cdot m^{-2} \cdot s^{-1}$]	q	heat flux [$W \cdot m^{-2}$]
g	generic quantity [-]	Q	thermal power exchanged [W]
H	fin height [m]	s	standard deviation [-]
h	heat transfer coefficient [$W \cdot m^{-2} \cdot K^{-1}$]	T	temperature [K]
h_{lv}	liquid vapor phase change enthalpy [$J \cdot kg^{-1}$]	x	refrigerant quality [-]
k	thermal conductivity [$W \cdot m^{-1} \cdot K^{-1}$]	Z	pressure drop per unit length [$Pa \cdot m^{-1}$]

Greek symbols

α	apex angle [°]	ΔT	temperature difference [K]
β	helix angle [°]	Δx	quality change in the test section [-]
$\Delta_{\%}$	percentage variation of a quantity [-]	μ	dynamic viscosity [$kg \cdot m^{-1} \cdot s^{-1}$]
Δp	pressure drop [Pa]	ρ	density [$kg \cdot m^{-3}$]

Subscripts

a	water	*o*	outlet
b	bottom	*r*	refrigerant
e	evaporator	*R*	fin root
i	inlet	*s*	side
lm	logarithmic mean	*sat*	saturation
m	mean	*t*	top

References

[1] The European Parliament and Council of the European Union, "European Regulation (EU) No. 517/2014," *Offiicial J. Eur. Union*, pp. 195–230, 2014.
[2] Hodnebrog *et al.*, "Global warming potentials and radiative efficiencies of halocarbons and related compounds: A comprehensive review," *Rev. Geophys.*, vol. 51, no. 2, pp. 300–378, 2013.
[3] G. Censi and A. Padovan, "R1234ze(E) As Drop-In Replacement For R134a In A Micro-Fin Shell-And-Tube Evaporator : Experimental Tests And Calculation Model Evaporator : Experimental Tests And Calculation Model," in *18th International Refrigeration and Air Conditioning Conference*, 2021.
[4] L. P. M. Colombo, A. Lucchini, and L. Molinaroli, "Experimental analysis of the use of R1234yf and R1234ze(E) as drop-in alternatives of R134a in a water-to-water heat pump," *Int. J. Refrig.*, vol. 115, pp. 18–27, 2020.
[5] J. Zhang, M. R. Kaern, T. Ommen, B. Elmegaard, and F. Haglind, "Condensation heat transfer and pressure drop characteristics of R134a, R1234ze(E), R245fa and R1233zd(E) in a plate heat exchanger," *Int. J. Heat Mass Transf.*, vol. 128, pp. 136–149, 2019.
[6] J. Y. Choi, M. A. Kedzierski, and P. A. Domanski, "Generalized Pressure Drop Correlation for Evaporation and Condensation in Smooth and Micro-Fin Tubes," *IIF-IIR-Commission B1*, no. 1 986, 2001.
[7] M. Goto, N. Inoue, and N. Ishiwatari, "Condensation and evaporation heat transfer of R410A inside internally grooved horizontal tubes," *Int. J. Refrig.*, vol. 24, no. 7, pp. 628–638, 2001.
[8] A. Cavallini, D. Del Col, L. Doretti, G. A. Longo, and L. Rossetto, "Heat transfer and pressure drop during condensation of refrigerants inside horizontal enhanced tubes Transfert de chaleur et chute de pression lors de la Á nes a Á l ' inte Â rieur de tubes condensation de frigorige Á surface augmente Âe horizontaux a," vol. 23, pp. 4–25, 2000.
[9] B. A. Shannak, "Frictional pressure drop of gas liquid two-phase flow in pipes," *Nucl. Eng. Des.*, vol. 238, no. 12, pp. 3277–3284, 2008.
[10] L. Sun and K. Mishima, "Evaluation analysis of prediction methods for two-phase flow pressure drop in mini-channels," *Int. Conf. Nucl. Eng. Proceedings, ICONE*, vol. 2, no. 15, pp. 649–658, 2008.
[11] S. Nozu, H. Katayama, H. Nakata, and H. Honda, "Condensation of a refrigerant CFC11 in horizontal microfin tubes (Proposal of a correlation equation for frictional pressure gradient)," *Exp. Therm. Fluid Sci.*, vol. 18, no. 1, pp. 82–96, 1998.
[12] H. Müller-Steinhagen and K. Heck, "A simple friction pressure drop correlation for two-phase flow in pipes," *Chem. Eng. Process. Process Intensif.*, vol. 20, no. 6, pp. 297–308, 1986.
[13] M. A. Kedzierski and J. M. Goncalves, "Horizontal convective consensation alternative refrigerants within a micro-fin tube," *Jorunal Enhanc. Heat Transf.*, vol. 6, no. 161–178, 1999.
[14] M. A. Akhavan-Behabadi, R. Kumar, and S. G. Mohseni, "Condensation heat transfer of R-134a inside a microfin tube with different tube inclinations," *Int. J. Heat Mass Transf.*, vol. 50, no. 23–24, pp. 4864–4871, 2007.
[15] J. Yu and S. Koyama, "Condensation heat transfer of pure refrigerants in microfin tubes," *Int. Refrig. Air Cond. Conf.*, 1998.
[16] A. Cavallini *et al.*, "Condensation in horizontal smooth tubes: A new heat transfer model for heat exchanger design," *Heat Transf. Eng.*, vol. 27, no. 8, pp. 31–38, 2006.
[17] L. P. M. Colombo, A. Lucchini, T. Nhan Phan, L. Molinaroli, and A. Niro, "Design and assessment of an experimental facility for the characterization of flow boiling of azeotropic refrigerants in horizontal tubes," *J. Phys. Conf. Ser.*, vol. 1224, no. 1, 2019.
[18] L. P. M. Colombo, A. Lucchini, L. Molinaroli, A. Niro, T. N. Phan, and P. G. Pittoni, "Flow patterns during flow boiling and convective condensation of R1234ze(E) inside a microfin tube," *5-6th Therm. Fluids Eng. Conf.*, pp. 109–119, 2021.
[19] H. Müller-Steinhagen and K. Heck, "A simple friction pressure drop correlation for two-phase flow in pipes," *Chem. Eng. Process.*, vol. 20, no. 6, pp. 297–308, 1986.